

mechanisms (Fig. 2b, c; Fig. 3c). Third, as suggested for adrenal chromaffin cells²², Ca^{2+} influx could activate release of Ca^{2+} from internal stores that are distributed non-uniformly throughout the cytoplasm. But Cd^{2+} , a specific blocker of the L-type calcium current^{19,20}, reduced the L-type current and the change in $[Ca^{2+}]_i$ by the same extent (Fig. 3), inconsistent with this hypothesis. Thus it is highly likely that the hotspots we observed resulted from nonuniform clustering of L-type channels within the growth-cone membrane.

Although many studies have indicated a role for $[Ca^{2+}]_i$ in modulating growth-cone behaviour, the results are paradoxical. An increase in $[Ca^{2+}]_i$ can cause outgrowth of the growth-cone margin^{7,8}, but it also inhibits neurite elongation^{6,8}. Consistent with the hypothesis that $[Ca^{2+}]_i$ promotes localized margin outgrowth, we found that hotspots were usually located at the base of processes that had extended from the growth cone (for example, structures marked p in Fig. 2b). Out of 32 growth cones, 24 had processes. In these 24 growth cones, process bases comprised only 20% of the total circumference of the growth cone (measured as angles subtended at the growth-cone centre), but 38 hotspots out of a total of 47 were located at the process base, indicating a high spatial correlation ($P < 0.001$, χ^2 test). We observed hotspots in both proximal and distal regions of the growth cone. No hotspots were observed in the neurite (marked n in Figs 2b, and 4a), where raised $[Ca^{2+}]_i$ inhibits growth.

To examine the $[Ca^{2+}]_i$ changes produced under physiological conditions, we used a conventional microelectrode to pressure-inject Fura-2 and electrically stimulate cells (Fig. 4b) maintained in a medium containing 1.8 mM Ca^{2+} at 32–36 °C. Distinct Ca^{2+} hotspots could be detected during a train of five action potentials at 10 Hz (Fig. 4a). In two growth cones, hotspot $[Ca^{2+}]_i$ increased to $> 1 \mu M$ during the train (for example, Fig. 4c). On average, hotspot $[Ca^{2+}]_i$ increased by 89 ± 26 nM per action potential ($n = 11$); that is, 12 action potentials would be required to raise hotspot $[Ca^{2+}]_i$ to micromolar levels. In 7 of the 11 growth cones, we saw outgrowth of the growth-cone margin by $6 \pm 1 \mu m$ in the 4 min following action-potential stimulation. In five of these, the site at which the greatest outgrowth occurred was close to a hotspot, indicating a strong spatial correlation between hotspots and site of outgrowth ($P < 0.001$, χ^2 test; see Fig. 4 legend for details). $[Ca^{2+}]_i$ is thought to affect cell morphology by activating proteins that cut, nucleate and cap actin filaments^{5,23}. These proteins are activated by micromolar concentrations of $[Ca^{2+}]_i$. Our results demonstrate that at the hotspot, relatively few action potentials will raise $[Ca^{2+}]_i$ sufficiently to activate these proteins.

The results described here could explain how the pattern of connections formed in the developing nervous system depends on the electrical activity in the neurons²⁴. Unstimulated growth cones tend to grow straight forwards²⁵. But hotspots, and therefore the margin outgrowth caused by electrical activity, are asymmetric. $[Ca^{2+}]_i$ hotspots produced by clustering of L-type Ca^{2+} channels therefore provide a mechanism for triggering the turning of electrically active neurites, and could have a crucial role during development.

Note added in proof. Consistent with the identification of the hotspot calcium channels as L-type and not N-type, the dihydropyridine agonist BAY K8644 (1 μM) enhanced the L-type current by $170 \pm 14\%$ ($n = 8$), but had no effect on the T-type current.

13. Lipscombe, D. et al. *Proc. natn. Acad. Sci. U.S.A.* **85**, 2398–2402 (1988).
14. Thompson, S. & Coombs, J. *J. Neurosci.* **8**, 1929–1939 (1988).
15. Fox, A. P., Nowycky, M. C. & Tsien, R. W. *J. Physiol.* **394**, 173–200 (1987).
16. Jones, O. T., Kunze, D. L. & Angelides, K. *J. Science* **244**, 1189–1193 (1989).
17. Pumplin, D. W., Reese, T. S. & Linas, R. *Proc. natn. Acad. Sci. U.S.A.* **78**, 7210–7213 (1981).
18. Bolsover, S. R. *J. gen. Physiol.* **88**, 149–165 (1986).
19. Narahashi, T., Tsunoo, A. & Yoshii, M. *J. Physiol.* **383**, 231–249 (1987).
20. Tsien, R. W., Lipscombe, D., Madison, D. V., Bley, K. R. & Fox, A. P. *Trends Neurosci.* **11**, 431–438 (1988).
21. Nowycky, M. C., Fox, A. P. & Tsien, R. W. *Nature* **316**, 440–443 (1985).
22. O'Sullivan, A. J., Cheek, T. R., Moreton, R. B., Berridge, M. J. & Burgoyne, R. D. *EMBO J.* **8**, 401–411 (1989).
23. Cooper, J. A. et al. *J. Cell Biol.* **104**, 491–501 (1987).
24. Purves, D., Lichtman, J., W. *Principles of Neural Development* (Sinauer, Sunderland, Massachusetts, 1985).
25. Gundersen, R. W. & Barrett, J. M. *J. Cell Biol.* **87**, 546–554 (1980).
26. Grynkiewicz, G., Poenie, M. & Tsien, R. Y. *J. biol. Chem.* **260**, 3440–3540 (1975).
27. Lansman, J. B., Hess, P. & Tsien, R. W. *J. gen. Physiol.* **88**, 321–347 (1986).

ACKNOWLEDGEMENTS. This work was supported by the Wellcome Trust and the MRC. We thank Drs M. Whitaker, D. Attwell and B. Barbour for discussion of the manuscript.

Homing of a $\gamma\delta$ thymocyte subset with homogeneous T-cell receptors to mucosal epithelia

Shigeyoshi Itohara, Andrew G. Farr*, Juan J. Lafaille, Marc Bonneville, Yohtaroh Takagaki, Werner Haas† & Susumu Tonegawa

Howard Hughes Medical Institute at Center for Cancer Research, and Department of Biology, Massachusetts Institute of Technology, Cambridge, Massachusetts 02139, USA

Department of Biological Structure SM-20, University of Washington, Seattle, Washington 98185, USA

† Hoffman La Roche Co. Ltd, Grenzacherstrasse 487, CH-4005 Basel, Switzerland

In mice $\gamma\delta$ T-cell populations with distinct T-cell receptor (TCR) repertoires and homing properties have been identified. Diversified populations are found in lymphoid organs^{1–3} and intestinal epithelia^{4,5}. By contrast, the $\gamma\delta$ T-cells that have been found in the murine skin are homogeneous. They express a TCR consisting of one particular V γ 5 and one particular V δ 1 chain^{5,6} and seem to originate from early fetal thymocytes^{6,7}. We have now systematically analysed many tissues by immunohistochemistry and TCR gene sequencing aided by the polymerase chain reaction. These studies revealed a second homogeneous $\gamma\delta$ T-cell subset in epithelia not of the intestine and skin, but of the vagina, uterus and tongue. The TCR expressed by this $\gamma\delta$ T-cell subset consists of the same V δ 1 chain. Cells that express this particular TCR have previously been shown to be positively selected in the late fetal thymus⁷.

We performed immunohistological analysis using monoclonal antibody 3A10 (ref. 8) on frozen tissue sections of various organs from 8–10-week-old BALB/c mice. We found $\gamma\delta$ T cells in most of the tissues analysed, frequently in close association with epithelial cells (Table 1). Representative data of tongue, vagina and uterus, which are discussed here, are shown in Fig. 1a. Most $\gamma\delta$ T cells in tongue and vagina were attached to, or embedded in, the basal layer of stratified squamous epithelium (Fig. 1a). About 30% of $\gamma\delta$ T cells in uterus were associated with simple columnar luminal epithelium (Fig. 1a). The rest of uterine $\gamma\delta$ T cells were broadly distributed in endometrium and myometrium (Fig. 1a, and data not shown). Staining of adjacent sections with monoclonal antibody H57-597 (ref. 9) showed that some $\alpha\beta$ T cells were also present in most tissues, but they were mainly distributed in subepithelial regions (Fig. 1a, and data not shown). $\gamma\delta$ T cells seemed to be localized to all epithelia that faced internal or external body surfaces, but not to epithelia within organs such as kidney, pancreas, liver or testis (Table 1).

To determine the use of V γ gene segments, we extracted DNA from lymphocyte preparations of various tissues of C57BL/6 mice (8–10-weeks old) and amplified it by the polymerase chain

Received 24 October; accepted 21 December 1989.

1. Smith, S. J., MacDermott, A. B. & Weight, F. F. *Nature* **304**, 350–352 (1983).
2. Neering, J. R. & McBurney, R. N. *Nature* **309**, 158–160 (1984).
3. Bolsover, S. R. & Spector, I. *J. Neurosci.* **6**, 1934–1940 (1986).
4. Baker, P. F. & Knight, D. E. *Phil. Trans. Roy. Soc. B296*, 83–103 (1981).
5. Manalan, A. S. & Klee, C. B. *Adv. Cyclic Nucleotide* **18**, 227–278 (1984).
6. Mattson, M. P. & Kater, S. B. *J. Neurosci.* **7**, 4034–4043 (1987).
7. Goldberg, D. J. *J. Neurosci.* **8**, 2596–2605 (1988).
8. Silver, R. A., Lamb, A. G. & Bolsover, S. R. *J. Neurosci.* **9**, 4007–4020 (1989).
9. Kater, S. B., Mattson, M. P., Cohan, C. & Connor, J. *Trends Neurosci.* **11**, 315–321 (1988).
10. Smith, S. J. & Augustine, G. J. *Trends Neurosci.* **11**, 458 (1988).
11. Tank, D. W., Sugimori, M., Connor, J. A. & Llinas, R. R. *Science* **242**, 773–777 (1988).
12. Regehr, W. G., Connor, J. A. & Tank, D. W. *Nature*, **341**, 533–536 (1989).

reaction (PCR)¹⁰ using primers for *Jγ1* and various *Vγ*-segments. We detected the amplified DNA by Southern-blot analysis using a *Jγ1*-specific oligonucleotide probe (Fig. 2a). We determined the relative intensity of the bands by using a Fuji Bioimage Analyser and converted this to the relative frequency of the corresponding rearrangement in a given DNA sample by using the standardization curves shown in Fig. 2b. As expected from previous studies, *Vγ4*, *Vγ5* and *Vγ7* were preferentially used by $\gamma\delta$ T cells in peripheral lymphoid organs, skin and small intestine, respectively (Fig. 2a)⁴⁻⁶. It was of interest that *Vγ6-Jγ1* rearrangements, which predominate in the fetal and newborn thymocyte preparations (Fig. 2a, compare the ratio of *Vγ4* and *Vγ6* bands of fetal and adult thymus)^{7,11,12} predominated in lymphocyte preparations from the tongue, uterus and vagina, although some *Vγ4-Jγ1* rearrangements, and very few *Vγ7-Jγ1*, *Vγ5-Jγ1* (Fig. 2a) and *Vγ1-Jγ4* rearrangements (data not shown), were also observed in these T cells. Flow cytometric analysis of lymphoid cell suspension from these tissues showed that about half of the cells carrying the CD3 antigen were $\gamma\delta^+$ TCR, Thy-1⁺, CD4⁻ and CD8⁻ (Fig. 1b). Few if any of these cells could have been derived from 'contaminating' blood, because only 3% of CD3⁺ blood cells express $\gamma\delta$ TCRs⁸.

TABLE 1 Distribution of $\gamma\delta$ T cells in mouse

Organs	Presence of $\gamma\delta$ T cells*	Contact with epithelial cells	No. of cells per animal†
Digestive system			
Tongue	+	+	
Oesophagus	+/- ‡	+	
Stomach	+	+	
Small intestine	+	+	1 × 10 ⁶
Large intestine	+	+	1 × 10 ⁵
Liver	-		
Pancreas	-		
Reproductive system			
Ovary	+/-		
Uterus	+	+	1 × 10 ⁵
Vagina	+	+	1 × 10 ⁵
Testis	-		
Epididymis	+/-	-	
Urinary system			
Kidney	-		
Bladder	+	+	
Others			
Skin	+	+	5 × 10 ⁶
Brain	-		
Heart	-		
Lymphoid organs			
Thymus	+		1 × 10 ⁶
Spleen	+		8 × 10 ⁵
Lymph-node	+		1 × 10 ⁵
Blood	+		6 × 10 ⁴

* The data from BALB/c mice examined by immunohistological experiments except for blood.

† The numbers of $\gamma\delta$ T cells in lymphoid organs (C57BL/6) were determined by flow cytometry⁸. For other organs, the approximate numbers of $\gamma\delta$ T cells were estimated as follows: (number of $\gamma\delta$ T cells per cross section of the organ) × ((length of the organ in μm)/(thickness of the section (6 μm) × 2)). The calculation is based on the assumption that a stained T cell (~8 μm in diameter) observed would almost always occupy two adjacent tissue sections (each 6 μm thick). We also assume that the tissues or organs examined have a constant diameter.

‡ Very scarce distribution of $\gamma\delta$ T cells is indicated by +/-.

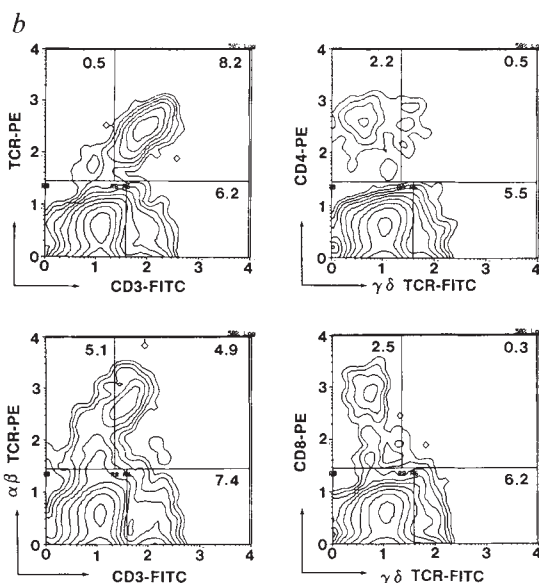
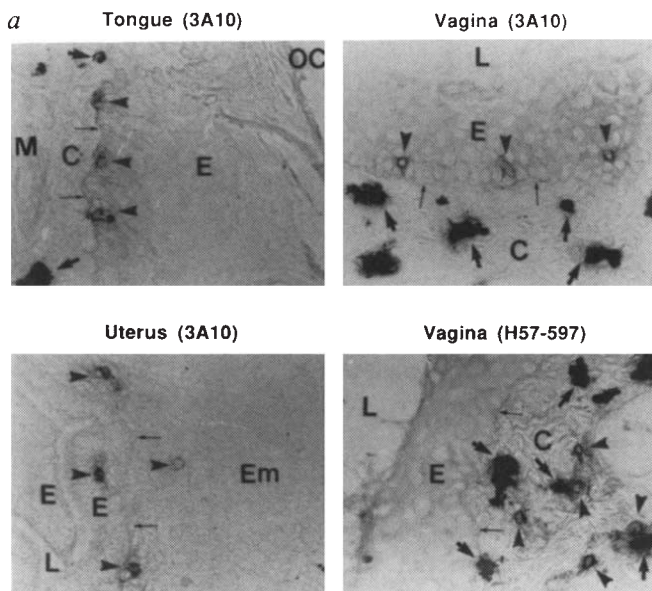


FIG. 1 Demonstration of $\gamma\delta$ T cells in tongue, vagina and uterus. *a*, Immunohistostaining of tissue sections. Fresh tissues from 8-to-10-week-old BALB/c mice were snap-frozen, and 6 μm sections were fixed with cold acetone, stained with a monoclonal antibody anti- $\gamma\delta$ TCR (3A10), or a monoclonal antibody anti- $\alpha\beta$ TCR (H57-597), affinity-purified goat anti-hamster IgG-biotin (Caltag, California), and avidin-horseradish peroxidase conjugates. The specificity of the staining was confirmed by the control staining of adjacent sections without the primary antibody. Arrowheads indicate some of the stained TCR-positive cells. Large and small arrows indicate endogenous peroxidase activity and basal lamina, respectively. E, epithelium; OC, oral cavity; L, lumen; M, striated voluntary muscle; C, connective tissue; Em, endometrium. *b*, Flow cytometric analysis of lymphocytes prepared from reproductive organs. Conjugates of anti-CD3(145-2C11)-fluorescein isothiocyanate (FITC), anti- $\gamma\delta$ TCR(3A10)-biotin or -FITC, anti- $\alpha\beta$ TCR(H57-597)-biotin, anti-CD4(GK1.5)-phycoerythrin (PE), anti-CD8(53-6.7)-biotin, and streptavidin-PE. Quadrants were determined on the basis of the control staining with streptavidin-PE and a goat anti-hamster-FITC conjugate. The percentage of positive cells in each quadrant is shown. Fluorescence intensity is shown in \log_{10} scale.

METHODS. Vaginae and uteri from 10-week-old C57BL/6J mice were extensively washed with PBS, minced into ~1-mm³ pieces, and digested for 1 h with 0.5% trypsin and 0.02% EDTA in PBS. Lymphoid cells were pelleted by centrifugation through 30% Percoll (Pharmacia LKB, Sweden) at 1,750 r.p.m. for 10 min, washed, and incubated overnight at 37 °C in RPMI 1640 medium containing 10% FCS and lymphokines (interleukins-1 and -2). Nonadherent cells were collected and examined by procedures described previously⁸.

We cloned many *Vγ6-Jγ1* PCR products from these cells and determined the junctional sequences of randomly chosen clones. Most of these sequences were in-frame and identical with the canonical γ -chain gene sequence expressed by late fetal $\gamma\delta$ thymocytes⁷ (Fig. 2c). To confirm the identity of TCR expressed by the uterus- and vagina-associated $\gamma\delta$ T-cell subset with the late fetal $\gamma\delta$ thymocytes, we further cloned and sequen-

ced *Vδ1-Jδ2* PCR products prepared from the DNA isolated from this peripheral $\gamma\delta$ T-cell subset. Indeed, we found that the *Vδ1-Dδ2-Jδ2* sequence was identical to that used in the thymocytes (Fig. 2d)⁷. By contrast, most other sequenced *Vγ-Jγ* junctions in the same DNA preparations were out-of-frame. Therefore, all of four *Vγ5-Jγ1* sequences were out of frame, and only four of twenty *Vγ4-Jγ1* sequences were in-frame, and

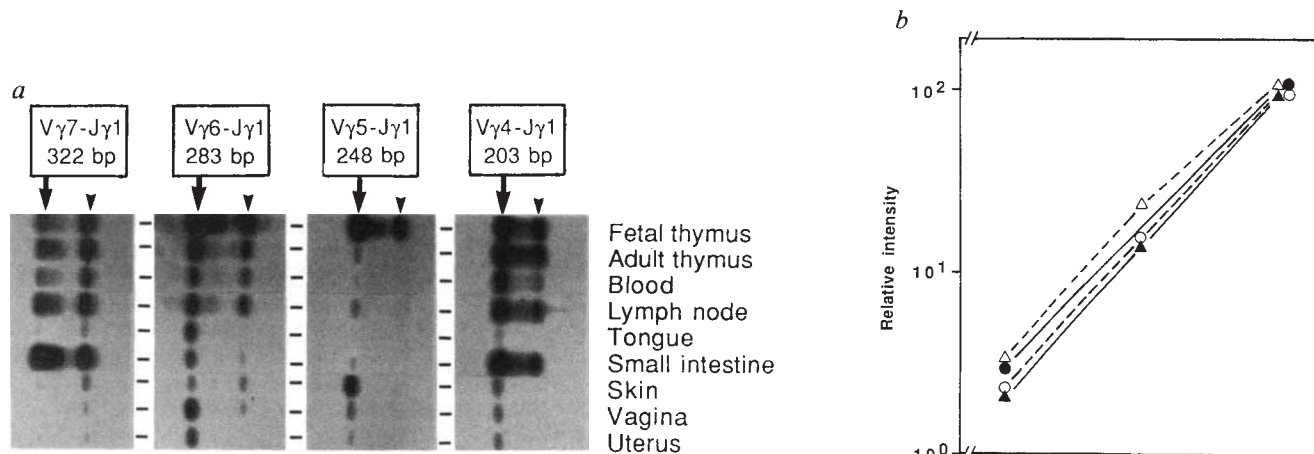


FIG. 2 a, Detection of rearranged TCR γ -chain gene segments in various organs by Southern-blot analysis of PCR-amplified products of chromosomal DNA. The blots of PCR products were probed with a *Jγ1*-specific oligonucleotide probe. The expected length of the respective PCR product from previously characterized $\gamma\delta$ T-cell hybridomas (V4, KN6; V5, KI129; V6, KI21; and V7, KN106)^{3,12} is indicated by the arrows. The arrowheads indicate dimeric products which could have formed using the imperfect inverted repeats within the *Jγ*-gene segment. b, Standardization curves of PCR reactions. The control experiments using serial dilutions of DNA from the hybridomas indicated that the intensity of PCR bands is proportional to the copy number of the corresponding genes. \circ , *Vγ4-Jγ1*; \bullet , *Vγ5-Jγ1*; Δ , *Vγ6-Jγ1*; \blacktriangle , *Vγ7-Jγ1*. c, *Vγ-Jγ1* junctional sequences in female reproductive organs (uterus and vagina) and tongue. d, *Vδ1-Dδ2-Jδ2* junctional sequences are aligned with germline sequences of *Vγ* and *Jγ1*^{4,7,11}, *Dδ2* and *Jδ2*¹⁹ gene segments. *V-J* or *V-D-J* joining can be either compatible or incompatible with the translation of the *J* segment in a required frame. This is indicated for each junctional sequence. The sequences indicated by asterisks are identical with the canonical sequence observed in the *Vγ6* subset of fetal thymocytes⁷. The in-frame *Vγ4* clone indicated by parenthesis cannot encode a complete γ -chain, because of the termination codon (TAA, underlined) present in the *Vγ4* gene segment. Also shown is the frequency of DNA clones obtained for each junctional sequence.

METHODS. Cells were prepared from the lymphoid organs, skin and intestines as previously described^{4,5}. Cells from the other epithelia were prepared by digestion with trypsin followed by centrifugation as described in the legend to Fig. 1. These samples still contain large numbers of nonlymphoid cells. High relative molecular mass DNA was extracted, digested with *EcoRI*, and subjected to PCR. The PCR primers used were: *Vγ4*, 5'-TGTCTTGCACCCCTACCC-3'; *Vγ5*, 5'-TGTGCACTGGTACCACTGA-3'; *Vγ6*, 5'-AGTGTTCAGAAAGCCCGATGC-3'; *Vγ7*, 5'-AAGCTAGAGGGGTCTCTGC-3'; and *Jγ1*, 5'-CAGAGGGAATTAATCTATGAGC-3'; *Vδ1*, 5'-GAATGGAAC-TAATGCTCTGT-3'; and *Jδ2*, 5'-CAACTTACGGGCTCCAC-3'. Test DNA (2 μ g) was made up to 100 μ l in a reaction mixture (10 mM Tris-HCl buffer, pH 8.3, 50 mM KCl, 1.5 mM MgCl₂, 100 pmol both primers, 0.25 mM each dNTP, 0.01% gelatin, and 2.5 U *Taq* polymerase). Thirty PCR cycles were run with 1 min at 92 °C, 2 min at 50 °C for γ -chain genes, or at 45 °C for δ -chain

c

Germ line	<i>Vγ6</i>				N	<i>Jγ1</i>				Frame Frequency	
	TGC	TGG	GAT	A		AT	AGC	TCA	GGT	TTT	In*
Vagina & uterus	TGC	TGG	GAT		GGCTC GCCGAA	AGC	TCA	GGT	TTT	In*	12/14
	TGC	TGG	GAT	A		GGT	TTT	Out	1/14		
	TGC	TGG	GAT			T	Out	1/14			
Tongue	TGC	TGG	GAT		CTCA	AGC	TCA	GGT	TTT	In*	7/8
	TGC	TGG	GAT			AGC	TCA	GGT	TTT	Out	1/8

Germ line	<i>Vγ5</i>				N	<i>Jγ1</i>				Frame Frequency		
	TGC	TGG	GAT	CT		AT	AGC	TCA	GGT	TTT	In*	Out
Vagina & uterus	TGC	TGG			AT	AT	AGC	TCA	GGT	TTT	Out	4/4

Germ line	<i>Vγ4</i>				N	<i>Jγ1</i>				Frame Frequency			
	TAC	GGC	<u>TAA</u>	AG		AT	AGC	TCA	GGT	TTT	In	Out	
Vagina & uterus	TAC	GGC			CGAT CAAGGG T A C CCGAT GAT GTAT CGAT AG T	AT	AGC	TCA	GGT	TTT	In	1/20	
	TAC	GGC	TA			T	AGC	TCA	GGT	TTT	In	1/20	
	TAC	GGC				GGT	TTT	In	1/20				
	TAC	GGC	<u>TAA</u>			AT	AGC	TCA	GGT	TTT	(In)	1/20	
	TAC	GG				AT	AGC	TCA	GGT	TTT	Out	5/20	
	TAC	GGC	<u>TAA</u>			T	AGC	TCA	GGT	TTT	Out	4/20	
	TAC	GGC	<u>TAA</u>	AG		C	AGC	TCA	GGT	TTT	Out	1/20	
	TAC	GGC				CCGAT	AT	AGC	TCA	GGT	TTT	Out	1/20
	TAC	GG				GAT	AT	AGC	TCA	GGT	TTT	Out	1/20
	TAC	GGC	T			GTAT	AT	AGC	TCA	GGT	TTT	Out	1/20
	TAC	GG				CGAT	AT	AGC	TCA	GGT	TTT	Out	1/20
	TAC	GGC	<u>TAA</u>	AG		AG	AGC	TCA	GGT	TTT	Out	1/20	
TAC	GGC	TA		T	AT	AGC	TCA	GGT	TTT	Out	1/20		

d

Germ line	<i>Vδ1</i>		N	<i>Dδ2</i>		N	<i>Jδ2</i>		Frame Frequency		
	TCA	GAT		ATCGGAGGGATACGAG	C		TCC	TGG	In*	Out	
Vagina & uterus	TCA	GAT		ATCGGAGGGGA		G	C	TCC	TGG	In*	6/6

genes, and 3 min at 72 °C per cycle. The PCR products were analysed by the Southern-blot hybridization technique previously described⁴. A *Jγ1* oligonucleotide, 5'-TGAATTCCTCTGCAAATACCTTG-3', end-labelled with ³²P was used as a probe. Autoradiograms were generated using the FUJI BA100 Bio-image analyzer (FUJI Photo Film Co. Ltd.). To make the standardization curves, the hybridoma DNAs were serially diluted with a DNA solution (2 μ g per 100 μ l) derived from the PCC3 embryonal carcinoma cell line²⁰ lacking any TCR γ -gene rearrangement, and were subjected to PCR reaction and Southern-blot hybridization. The intensities of autoradiographic bands were quantitated using the Fuji Bioimage Analyzer, and were plotted on a log scale. We estimated copy numbers of rearranged *Vγ* gene segments in a given test sample from the standardization curves. The preference of a particular *Vγ-Jγ1* rearrangement was estimated from the ratio of copy numbers of rearranged *Vγ-Jγ1* segments for each sample. The PCR products were purified, cloned and sequenced according to the procedure described elsewhere⁷.

one of these contained a premature termination codon in the 3' end of the V γ 4 segment (Fig. 2c). V γ 6 rearrangements also occur in many other tissues (Fig. 2a). But in all cases that have been studied in detail, the junctional sequences are different from the canonical sequence. For instance, 12 V γ 6-J γ 1 junctions from lymph node cells (this study, data not shown) and 8 V γ 6-J γ 1 junctions from intestinal epithelial lymphocytes (ref. 5; V γ 4-J γ 1 in the nomenclature used therein) were diverse, and none was identical with the canonical sequence. Therefore, homing to epithelia of vagina, uterus and tongue does not seem to be a property of all cells expressing V γ 6, but a property of cells expressing the canonical V γ 6-V δ 1 sequences.

The study described here shows that in mice, many peripheral $\gamma\delta$ T cells are localized in epithelia not only of the skin and the intestine, but also of several other mucosae that face body surfaces. These observations support the view that $\gamma\delta$ T cells play a part in the surveillance of body surfaces that are exposed to environmental hazards^{13,14}. It is of interest that the TCR repertoires of $\gamma\delta$ T cells differ in various tissues. Most intriguingly, two epithelium-associated $\gamma\delta$ T-cell subsets have distinct and homogeneous subsets of TCR, one in the skin^{5,6} and, as shown here, one in mucosal epithelia or organs such as vagina, uterus and tongue. Both subsets seem to originate from positive cellular selection in the fetal thymus⁷. The homing of these $\gamma\delta$ T-cells to epithelial sites could be mediated by TCR. But this possibility is neither very attractive nor consistent with the epithelial homing of $\gamma\delta$ T-cells with 'wrong receptors' observed in transgenic mice¹⁵. It is also unlikely that the localization of a given $\gamma\delta$ T-cell subset results from its specific retention in certain epithelia rather than by specific homing¹⁵. It is more likely that the two monospecific cell populations represent distinct $\gamma\delta$ T-cell sublineages differing not only in their TCR, but also in homing receptors and possibly other properties. One or both sublineages could be absent, or have different properties in other species such as man, in which a close association of $\gamma\delta$ T-cells with epidermal and mucosal epithelial cells has not been observed¹⁶⁻¹⁸. Each of the monospecific subset of $\gamma\delta$ T-cells in mice must recognize a self-component that selects these cells in the fetal thymus⁷ and regulates their function in the periphery; here the subset would be expressed in response to a large variety of pathogens or non-infectious agents, as previously speculated^{13,14}. Further study should shed light on the role of these epithelia-associated $\gamma\delta$ T-cell subsets in the immune system. □

Received 27 October; accepted 22 December 1989.

- Elliott, J. F., Rock, E. P., Patten, P. A., David, M. M. & Chien, Y.-H. *Nature* **331**, 627-631 (1988).
- Lacy, M. J., McNeill, L. K., Roth, M. E. & Kranz, D. M. *Proc. natn. Acad. Sci. U.S.A.* **86**, 1023-1026 (1989).
- Takagaki, Y., Nakanishi, N., Ishida, I., Kanagawa, O. & Tonegawa, S. *J. Immunol.* **142**, 2112-2121 (1989).
- Takagaki, Y., DeCloux, A., Bonneville, M. & Tonegawa, S. *Nature* **339**, 712-714 (1989).
- Asanow, D. M., Goodman, T., Lefrancois, L. & Allison, J. P. *Nature* **341**, 60-62 (1989).
- Asanow, D. M. *et al. Cell* **55**, 837-847 (1988).
- LaFaille, J. J., DeCloux, A., Bonneville, M., Takagaki, Y. & Tonegawa, S. *Cell* **59**, 859-870 (1989).
- Itohara, S., Nakanishi, N., Kanagawa, O., Kubo, R. & Tonegawa, S. *Proc. natn. Acad. Sci. U.S.A.* **86**, 5094-5098 (1989).
- Kubo, R., Born, W., Kappler, J. W., Marrack, P. & Pigeon, M. *J. Immunol.* **142**, 2736-2742 (1989).
- Saiki, R. *et al. Science* **239**, 487-491 (1988).
- Garman, R. D., Doherty, P. J. & Raulet, D. H. *Cell* **45**, 733-742 (1986).
- Ito, K. *et al. Proc. natn. Acad. Sci. U.S.A.* **86**, 631-635 (1989).
- Janeway, C. A. Jr *Nature* **333**, 804-806 (1988).
- Janeway, C. A. Jr, Jones, B. & Hayday, A. *Immun. Today* **9**, 73-76 (1988).
- Bonneville, M. *et al., J. exp. Med.* (in the press).
- Groh, V. *et al. J. exp. Med.* **169**, 1277-1279 (1989).
- Bucy, P. R., Chen, C.-L. & Cooper, M. D. *J. Immunol.* **142**, 3045-3047 (1989).
- Brandtzaeg, P. *et al.; Bucy, R. P.; Vroom, T. M.; Bos, J. D.; Borst, J.; Janeway, C. A. Jr Nature* **341**, 113-114 (1989).
- Chien, Y.-H. *et al. Nature* **330**, 722-727 (1987).
- Jacob, H., Boon, T., Gaillard, J. & Jacob, F. *Ann. Microbiol. (Inst. Pasteur)* **124B**, 269-282 (1973).

ACKNOWLEDGEMENTS. We thank Suzanne Hoier and Andrew Nelson for technical assistance, Ralph Kubo for monoclonal antibody H57-597, Jeffrey A. Bluestone for monoclonal antibody 145-2C11, Antonio Coutinho and Charles A. Janeway, Jr for discussions, and Ely Basel and Gerry Kemske for typing the manuscript. This work was supported by the NIH (A.F. and S.T.); the Howard Hughes Medical Institute, the American Cancer Society and Ajinomoto Co. Ltd. (S.T.); Conselho Nacional de Pesquisas, Brazil (J.J.L.); and Ligue Nationale Contre le Cancer and Association pour la Recherche contre le Cancer (M.B.). We also thank Fuji Photo Film Co. for the use of the BA100-Bioimage Analyzer.

Rapid neutrophil adhesion to activated endothelium mediated by GMP-140

Jian-Guo Geng*, Michael P. Bevilacqua†, Kevin L. Moore*, Thomas M. McIntyre‡, Stephen M. Prescott‡, Jenny M. Kim†, Greg A. Bliss*, Guy A. Zimmerman‡ & Rodger P. McEver*§

* St Francis Medical Research Institute and Department of Medicine, University of Oklahoma Health Sciences Center and Cardiovascular Biology Research Program, Oklahoma Medical Research Foundation, 825 NE 13th Street, Oklahoma City, Oklahoma 73104, USA

† Vascular Research Division, Department of Pathology, Brigham and Women's Hospital and Harvard Medical School, Boston, Massachusetts 02115, USA

‡ Nora Eccles Harrison Cardiovascular Research and Training Institute and the Departments of Medicine and Biochemistry, University of Utah School of Medicine, Salt Lake City, Utah 84112, USA

GRANULE membrane protein-140 (GMP-140), a membrane glycoprotein of platelet¹⁻⁵ and endothelial cell⁶⁻⁸ secretory granules, is rapidly redistributed to the plasma membrane during cellular activation and degranulation^{1,2,6,7}. Also known as PADGEM protein⁴, GMP-140 (ref. 9) is structurally related to two molecules involved in leukocyte adhesion to vascular endothelium: ELAM-1, a cytokine-inducible endothelial cell receptor for neutrophils¹⁰, and the MEL-14 lymphocyte homing receptor^{11,12}. These three proteins define a new gene family, termed selectins, each of which contains an N-terminal lectin domain, followed by an epidermal growth factor-like module, a variable number of repeating units related to those in complement-binding proteins, a transmembrane domain, and a short cytoplasmic tail. Here we demonstrate that GMP-140 can mediate leukocyte adhesion, thus establishing a functional similarity with the other selectins. Human neutrophils and promyelocytic HL-60 cells bind specifically to COS cells transfected with GMP-140 complementary DNA and to microtitre wells coated with purified GMP-140. Cell binding does not require active neutrophil metabolism but is dependent on extracellular Ca²⁺. Within minutes after stimulation with phorbol esters or histamine, human endothelial cells become adhesive for neutrophils; this interaction is inhibited by antibodies to GMP-140. Thus, GMP-140 expressed by activated endothelium might promote rapid neutrophil targeting to sites of acute inflammation.

COS cells transfected with a cDNA encoding GMP-140 support adhesion (rosette formation) of isolated human neutrophils and promyelocytic HL-60 cells: similar adhesion has been observed with ELAM-1-transfected COS cells¹⁰. Immunoperoxidase analysis indicates that the anti-GMP-140 monoclonal antibodies G1, G2, S12 (refs 1, 5) and W40 (ref. 5) identify GMP-140-transfected COS cells, but not COS cells transfected with ELAM-1 or ICAM-1 cDNAs. Figure 1 shows that antibody G1 blocks adhesion of HL-60 cells to GMP-140-transfected COS cells, but not to ELAM-1-transfected COS cells. Conversely, anti-ELAM-1 antibody H18/7 (ref. 13) inhibits binding of HL-60 cells to COS cells expressing ELAM-1, but not to COS cells expressing GMP-140; there is a comparable specific inhibition of neutrophil adhesion. Leukocyte adhesion to GMP-140-transfected COS cells is also inhibited by G2, but not by S12 or W40, suggesting that these two antibodies recognize epitopes not essential for leukocyte binding.

Figure 2 shows that human neutrophils and HL-60 cells bind to microtitre wells coated with purified platelet GMP-140, but not to wells coated with control proteins. This indicates that GMP-140 is sufficient to promote leukocyte adhesion. Neutrophil binding is blocked by preincubation of GMP-140-

§ To whom correspondence should be addressed.